



This is a repository copy of *VAMP4 directs synaptic vesicles to a pool that selectively maintains asynchronous neurotransmission*.

White Rose Research Online URL for this paper:  
<http://eprints.whiterose.ac.uk/108268/>

Version: Accepted Version

---

**Article:**

Raino, J., Khvotchev, M., Liu, P. et al. (8 more authors) (2012) VAMP4 directs synaptic vesicles to a pool that selectively maintains asynchronous neurotransmission. *Nature Neuroscience*, 15 (5). pp. 738-745. ISSN 1097-6256

<https://doi.org/10.1038/nn.3067>

---

**Reuse**

Unless indicated otherwise, fulltext items are protected by copyright with all rights reserved. The copyright exception in section 29 of the Copyright, Designs and Patents Act 1988 allows the making of a single copy solely for the purpose of non-commercial research or private study within the limits of fair dealing. The publisher or other rights-holder may allow further reproduction and re-use of this version - refer to the White Rose Research Online record for this item. Where records identify the publisher as the copyright holder, users can verify any specific terms of use on the publisher's website.

**Takedown**

If you consider content in White Rose Research Online to be in breach of UK law, please notify us by emailing [eprints@whiterose.ac.uk](mailto:eprints@whiterose.ac.uk) including the URL of the record and the reason for the withdrawal request.



[eprints@whiterose.ac.uk](mailto:eprints@whiterose.ac.uk)  
<https://eprints.whiterose.ac.uk/>



Published in final edited form as:

*Nat Neurosci.* ; 15(5): 738–745. doi:10.1038/nn.3067.

## VAMP4 directs synaptic vesicles to a pool that selectively maintains asynchronous neurotransmission

Jesica Raingo<sup>1,2,\*</sup>, Mikhail Khvotchev<sup>1,\*</sup>, Pei Liu<sup>1,\*</sup>, Frederic Darios<sup>3</sup>, Ying C. Li<sup>1</sup>, Denise M.O. Ramirez<sup>1</sup>, Megumi Adachi<sup>4</sup>, Philippe Lemieux<sup>5</sup>, Katalin Toth<sup>5</sup>, Bazbek Davletov<sup>3</sup>, and Ege T. Kavalali<sup>1,6</sup>

<sup>1</sup>Department of Neuroscience, UT Southwestern Medical Center, Dallas, TX 75390-9111, USA

<sup>2</sup>Electrophysiology Laboratory, Multidisciplinary Institute of Cellular Biology, Calle 526 s/n, La Plata 1900, Buenos Aires, Argentina

<sup>3</sup>MRC Laboratory of Molecular Biology, Cambridge CB2 0QH, UK

<sup>4</sup>Department of Psychiatry, UT Southwestern Medical Center, Dallas, TX 75390-9111, USA

<sup>5</sup>Centre de recherche Université Laval Robert-Giffard, F-6500, 2601 Chemin de la Canardière Québec G1J 2G3, Canada

<sup>6</sup>Department of Physiology, UT Southwestern Medical Center, Dallas, TX 75390-9111, USA

### Abstract

Synaptic vesicles in the brain harbor several SNARE proteins. With the exception of synaptobrevin2/VAMP2 (syb2) that is directly involved in vesicle fusion, the role of these SNAREs in neurotransmission is unclear. Here, we show that in mice while syb2 drives rapid Ca<sup>2+</sup>-dependent synchronous neurotransmission, the structurally homologous SNARE protein VAMP4 selectively maintains bulk Ca<sup>2+</sup>-dependent asynchronous release. At inhibitory nerve terminals, up- or down-regulation of VAMP4 causes a correlated change in asynchronous release. Biochemically, VAMP4 forms a stable complex with SNAREs syntaxin-1 and SNAP-25 that does not interact with complexins or synaptotagmin-1, proteins essential for synchronous neurotransmission. Optical imaging of individual synapses indicates that VAMP4 and syb2 trafficking show minimal overlap. Taken together, these findings suggest that VAMP4 and syb2 diverge functionally, traffic independently and support distinct forms of neurotransmission. These

Users may view, print, copy, download and text and data- mine the content in such documents, for the purposes of academic research, subject always to the full Conditions of use: [http://www.nature.com/authors/editorial\\_policies/license.html#terms](http://www.nature.com/authors/editorial_policies/license.html#terms)

Correspondence should be addressed to: Ege T. Kavalali, Ph.D., Department of Neuroscience, U.T Southwestern Medical Center, 5323 Harry Hines Blvd., Dallas, TX 75390-9111, Phone: 214-648-1682, Fax: 214-648-1801, Ege.Kavalali@UTSouthwestern.edu.

\*These authors have equally contributed to this work.

### Contributions

JR, MK, and PL (Liu) conducted the majority of the experiments presented in the manuscript. FD and BD conducted the biochemical analysis presented in Figure 5 and Supplementary Figure 8 and contributed to the corresponding sections of manuscript. YCL and DMOR conducted the dual color imaging experiments. MA provided essential assistance with mouse breeding and genotyping. PL (Lemieux) and KT conducted immunoelectronmicroscopy and immunohistochemistry experiments (Figure 1 and Supplementary Figure 1&2) and contributed to the corresponding sections of manuscript. JR, MK and ETK conceptualized and planned the study. ETK wrote the paper.

### Competing financial interests

The authors declare no competing financial interests.

results provide molecular insight into how synapses diversify their release properties by taking advantage of distinct synaptic vesicle-associated SNAREs.

---

## Introduction

In the brain, fast synaptic transmission is mediated by the formation of SNARE (soluble NSF attachment protein receptor) complexes<sup>1</sup> containing the SNARE proteins syb2, syntaxin 1, and SNAP-25<sup>2-4</sup>. Although genetic deletion of any of these key SNAREs largely abolishes fast synchronous neurotransmitter release, significant levels of spontaneous neurotransmission and asynchronous release, which are loosely coupled to presynaptic Ca<sup>2+</sup> fluctuations, remain intact<sup>5-7</sup>. These findings imply the existence of non-canonical SNARE proteins involved in synaptic vesicle fusion that may preferentially support asynchronous or spontaneous neurotransmission<sup>6</sup>. Here, to address the molecular mechanisms that govern this heterogeneity of synaptic output, we examined the functional divergence of two vesicle-associated SNARE proteins, syb2 and VAMP4. Vesicle-associated SNAREs (v-SNAREs) are attractive substrates for such heterogeneity as they may nucleate distinct fusion complexes with differential contributions of key partners such as synaptotagmins, complexins and Munc18, and thus diversify neurotransmitter release patterns<sup>8</sup>.

Syb2 and VAMP4 are v-SNAREs both present on synaptic vesicles within central synapses<sup>9</sup>. Whereas syb2 is mostly restricted to vesicles, VAMP4 has a broader subcellular distribution and is also implicated in endosomal and trans-Golgi network vesicle trafficking<sup>10, 11</sup>. Syb2 and VAMP4 are highly homologous in their SNARE motifs and C-terminal regions, but possess unique N-terminal sequences. VAMP4 has a longer N-terminal region, which contains a di-leucine motif critical for its localization to the Golgi apparatus<sup>12</sup>. In this study, to uncover the role of VAMP4 in neurotransmitter release, we performed molecular analysis of VAMP4 in conjunction with high resolution electrophysiology and multicolor optical imaging. These experiments showed that while syb2 is involved in rapid Ca<sup>2+</sup>-dependent synchronous neurotransmission, the structurally homologous VAMP4 could selectively maintain bulk Ca<sup>2+</sup>-dependent asynchronous release as well as some spontaneous release. We also found that VAMP4 forms a stable complex with the plasma membrane SNAREs syntaxin-1 and SNAP-25. However, in contrast to syb2-containing SNARE complexes, these VAMP4-containing complexes do not readily interact with complexins or synaptotagmin 1, which are required for fast synchronous neurotransmitter release<sup>13-15</sup>. Multicolor optical imaging of individual synapses revealed that VAMP4 exocytosis and endocytosis had limited overlap with the trafficking of syb2. Taken together, these results support a model where activity-dependent generation of synaptic vesicles enriched in VAMP4 can specifically drive asynchronous release.

## Results

### Synaptic localization of VAMP4

To examine the putative role of VAMP4 in regulation of neurotransmission, we initially evaluated synaptic distribution of VAMP4 expression in the CA1 area of the hippocampus using immunocytochemistry. In agreement with previous work, we found that VAMP4 has a

broader subcellular distribution which gave rise to prominent immunofluorescence staining in the cell body layer (stratum pyramidale, s.p.) (Fig. 1a). This observation is consistent with its role in endosomal and trans-Golgi network vesicle trafficking as well as association with the Golgi apparatus located in cell bodies. However, we also observed punctate staining in every layer of the hippocampus including stratum radiatum (s.r.) and stratum oriens (s.o.), where apical and basal dendrites of pyramidal cells reside (Fig. 1a–b). Interestingly, some of this punctate staining showed co-localization with cholecystokinin (CCK) which labels synapses originating from a subset of inhibitory interneurons, that preferentially support asynchronous neurotransmitter release<sup>16</sup> (Fig. 1b–d arrows). Parvalbumin-positive inhibitory interneuron terminals, on the other hand, showed very limited presence of VAMP4, in contrast to its extensive distribution in adjacent pyramidal cell bodies (Supplementary Fig. 1). Ultrastructural analysis of nerve terminals (t) with silver-enhanced immunogold staining showed that VAMP4 was indeed present in presynaptic terminals suggesting a potential role in neurotransmitter release (Fig 1e, f). Synaptic localization of VAMP4 at the ultrastructural level followed a similar pattern to that of syb2, however, syb2 was clearly more abundant across terminals (Supplementary Fig. 2). We also conducted a similar immunocytochemical analysis of VAMP4 expression in dissociated hippocampal cultures. In this setting, we uncovered synaptic localization of VAMP4 at low levels (Supplementary Fig. 3) in addition to its association with neuronal somata (see also Supplementary Fig. 6).

### VAMP4 selectively rescues asynchronous neurotransmission

To examine the role of VAMP4 in neurotransmission, we tested the ability of VAMP4 to mediate neurotransmitter release in the absence of syb2. We employed high-density cultures of hippocampal neurons prepared from mouse embryos deficient in syb2<sup>6</sup> and focused on properties of inhibitory postsynaptic currents (IPSCs) which typically originate from parvalbumin-positive inhibitory interneurons present in this system (Supplementary Fig. 4). Here, it is important to note that to date we could not identify CCK expressing neurons in culture, this could be due to selective vulnerability of these neurons to dissociation or possible alterations in cell identity in culture. IPSCs were isolated after pharmacological blockade excitatory synaptic currents. This setting allowed us unambiguous dissection of synchronous, asynchronous and spontaneous forms of neurotransmission without contamination from background network activity triggered by excitatory glutamate release<sup>17</sup>. Lentivirus-mediated expression of VAMP4 resulted in significant levels of evoked neurotransmission in syb2-deficient neurons compared to non-infected controls, although the peak amplitudes of these field stimulation evoked IPSCs were substantially lower than those mediated by syb2 expression (Fig. 2a). This discrepancy was evident despite the fact that VAMP4 was reliably trafficked to most synaptic terminals that typically express syb2 (see below Fig. 6). Upon 10 Hz field stimulation, VAMP4-expressing synapses could sustain robust release after an initial phase of facilitation, whereas the high level of release maintained by syb2 showed rapid depression consistent with its relatively high release probability (Fig. 2b). The ratios of IPSCs evoked in response to paired pulse stimulation (P2/P1) showed a significant increase indicating the reduced release probability of synapses expressing VAMP4 (Supplementary Fig. 5). In VAMP4-expressing neurons, cumulative integration of total charge transfer during 5 seconds of 10 Hz stimulation showed ~50% of

total release compared to syb2 expressing synapses (Fig. 2b). Interestingly, although initial responses in the train of 10 Hz stimulation evoked IPSCs manifested limited variance (calculated 40 ms after IPSC onset), continued stimulation triggered substantial asynchronicity as indicated by a significant increase in variance (Fig. 2c). Syb2 expressing neurons, on the other hand, showed only mild desynchronization upon repetitive stimulation, where variance detected at the decaying phase of the evoked IPSCs remained significantly below the level seen after VAMP4 expression.

In contrast to action potential evoked  $\text{Ca}^{2+}$ -dependent neurotransmission, neurotransmitter release triggered in response to hypertonic stimulation, which does not require  $\text{Ca}^{2+}$  influx, was not rescued by VAMP4 expression to a level significantly above that seen in non-infected syb2-deficient neurons (Fig. 2d). Surprisingly, spontaneous neurotransmitter release detected in the absence of presynaptic action potentials (recorded in the presence of TTX) showed a significant increase upon VAMP4 expression although this increase was rather modest compared to the robust rescue of spontaneous release by expression of syb2 in syb2-deficient neurons (Fig. 2e)<sup>18</sup>.

To analyze the kinetics of  $\text{Ca}^{2+}$ -dependent evoked neurotransmission maintained by VAMP4, we incubated syb2-deficient neurons expressing VAMP4 or syb2 with the membrane permeable slow  $\text{Ca}^{2+}$  buffer EGTA-AM. EGTA-AM application did not significantly alter the properties of the first evoked IPSC in a train (Fig. 3a) but substantially inhibited the evoked neurotransmitter release mediated by VAMP4 in subsequent action potentials without significantly altering the properties of syb2-dependent evoked release at any time point (Fig. 3b). Thus, VAMP4 can selectively support evoked asynchronous neurotransmission that is triggered by increases in bulk cytoplasmic  $\text{Ca}^{2+}$  during repetitive stimulation, whereas syb2 maintains predominantly synchronous neurotransmitter release in response to rapid  $\text{Ca}^{2+}$  transients that are relatively insensitive to the slow  $\text{Ca}^{2+}$  buffer.

### VAMP4 levels control the extent of asynchronous release

To test the notion that the level of VAMP4 expression determines synchronicity of neurotransmitter release, we manipulated VAMP4 levels in both directions by lentiviral overexpression and RNAi-mediated knockdown. Overexpression of syb2 in wild type neurons did not significantly change the waveform or EGTA-AM sensitivity of neurotransmitter release detected during 10 Hz stimulation (Fig. 3c). In contrast, VAMP4 overexpression significantly altered the neurotransmitter release waveform during 10 Hz stimulation, marked by the loss of the distinct saw-tooth pattern suggesting a decrease in synchronicity of release (Fig. 3d). In addition, VAMP4 overexpression substantially increased the sensitivity of baseline release to brief EGTA-AM incubation, resulting in nearly 50% reduction in cumulative release over a 5 second period compared to syb2 overexpression (Fig. 3d). A progressive increase in asynchronicity after VAMP4 overexpression compared to syb2 overexpression was also evident upon close examination of individual evoked IPSC traces (Fig. 3e, f).

We achieved efficient knockdown of VAMP4 in hippocampal neurons using two lentiviral short hairpin RNA constructs that reduced VAMP4 mRNA levels by 80–90% (Supplementary Fig. 6) and dramatically decreased endogenous VAMP4 protein without

significantly affecting levels of other presynaptic proteins (Fig. 4a). However, this reduction in VAMP4 levels did not result in a significant alteration of release kinetics as indicated by near identical cumulative charge histograms of evoked IPSCs triggered during mild 1 Hz stimulation (Fig. 4b). This observation is consistent with the premise that in these synapses VAMP4 is not essential for maintenance of synchronous release that dominates at low to moderate stimulation frequencies<sup>19</sup>. In contrast, when we challenged synapses with a pre-stimulation of 600 action potentials applied at 20 Hz, loss of VAMP4 decreased the propensity of subsequent asynchronous release detected during 1 Hz stimulation (Fig. 4c). Here, cumulative charge histograms of individual evoked IPSCs revealed a significant increase in the rapid synchronous component of release, although this effect was more prominent in response to one of the knock down constructs (KD2) (Fig. 4c). In addition to alteration in evoked neurotransmission, the decrease in VAMP4 levels also impaired the frequency of mIPSCs detected at rest (in the presence of TTX, Control:  $1.1 \pm 0.1$  Hz, n=14; KD1:  $0.8 \pm 0.1$  Hz, n= 17; KD2:  $0.7 \pm 0.1$  Hz, n=10). This result agrees with the gain of function effect of VAMP4 expression on spontaneous release we detected on the background of syb2 deficient synapses (Fig. 2e) and suggests that VAMP4 may in part be involved in maintenance of spontaneous neurotransmission.

These observations suggest that at near physiological extracellular 2 mM  $\text{Ca}^{2+}$  neurotransmitter release from wild type hippocampal neurons shows limited asynchronicity and relatively poor sensitivity to EGTA-AM application or VAMP4 knock down unless synapses are challenged with a sustained train of action potentials<sup>19, 20</sup>. Next, we evaluated the impact of VAMP4 knockdown by increasing the extracellular  $\text{Ca}^{2+}$  concentration to 8 mM which is an alternative means to exacerbate bulk cytoplasmic  $\text{Ca}^{2+}$  and asynchronicity of release (Fig. 4d–g). In neurons infected with both VAMP4 knockdown constructs, we observed a notable reduction in asynchronous release detected at the end of the 5s long 10 Hz train stimulation (Fig. 4d, e), as well as a reduction in cumulative release detected during the 10 Hz train (Fig. 4f). Differences in the kinetics of delayed release were also detectable when we compared normalized traces (Fig. 4d). In contrast, amplitudes of initial synaptic responses were only modestly affected by VAMP4 knockdown (Fig. 4g) consistent with the notion that VAMP4, under normal conditions, helps maintain asynchronous release during repetitive activity.

### The ternary complex of VAMP4 with syntaxin 1/SNAP-25

To elucidate the molecular basis of VAMP4-mediated neurotransmitter release, we analyzed interactions of VAMP4 with critical proteins involved in vesicle fusion. First, we tested whether VAMP4 can form the tight SDS-resistant SNARE complex with neuronal syntaxin1 and SNAP-25. The SNARE motifs of VAMP4 and syb2 were equally efficient in formation of SDS-resistant complexes with SNARE motifs of syntaxin1 and SNAP-25 *in vitro* (Fig. 5a). It has recently become clear that the abundant synaptic proteins complexins and synaptotagmin 1 engage SNAREs during SNARE complex formation to confer high synchronicity of calcium entry and vesicle fusion<sup>8</sup>. We thus tested whether recombinant complexin 2, immobilized on Glutathione-Sepharose beads via a GST tag, can bind to preformed SNARE complexes containing VAMP4. Figure 5b shows that immobilized complexin2 efficiently retained SNARE complexes containing syb2, but not VAMP4. To

confirm this result, we preassembled recombinant SNARE complexes containing Syntaxin1, GST-SNAP-25 and either VAMP4 or syb2 on Glutathione-Sepharose beads and incubated them with detergent rat brain extract (Fig. 5c). The bound proteins were analyzed by immunoblotting. Endogenous complexins and synaptotagmin1 bound to the SNARE complex containing syb2, but failed to interact with the SNARE complex containing VAMP4 (Fig. 5c) suggesting that complexins and synaptotagmin 1 specifically target syb2-mediated membrane fusion. Interaction of SNARE complexes with complexins and synaptotagmin1 has been shown to be critical for synchronous neurotransmitter release. Loss of these key synaptic proteins causes a robust decrease in overall synchronous release but spares asynchronous neurotransmission<sup>13–15</sup>. Therefore, inability of SNARE complexes containing VAMP4 to bind complexins or synaptotagmin1 could underlie the asynchronous nature of release sustained by VAMP4.

### VAMP4 and syb2 trafficking show limited overlap

Our findings suggest that an increase in the abundance of VAMP4 relative to syb2 renders vesicles insensitive to rapid  $\text{Ca}^{2+}$  transients, thus restricting their role to asynchronous release. To test whether VAMP4 and syb2 are targeted to the same vesicle population, we monitored trafficking of synaptic vesicle pools that express VAMP4 and syb2 using fluorescence imaging in live neurons. To examine co-trafficking of syb2 and VAMP4 in individual terminals, we tagged syb2 with mOrange, a fluorescent DsRed variant with pH sensitivity similar to green pHluorin<sup>21</sup> whereas VAMP4 was tagged with classical super-ecliptic pHluorin<sup>22</sup> attached at the short region after the transmembrane domain, which faces the vesicle lumen (Fig. 6a). Imaging experiments in live neurons expressing both fluorescent SNARE proteins revealed significant overlap in red and green signals within the same puncta, similar to that observed when mOrange- and pHluorin-tagged syb2 constructs were co-expressed (Fig. 6b, c). In most terminals, application of 20 Hz stimulation caused robust endocytic trafficking (internalization) of VAMP4-pHluorin and simultaneous exocytic trafficking of syb2-mOrange, which closely resembled canonical exocytic trafficking of syb2-pHluorin (Fig. 6d–e). In some boutons, we could detect a net exocytic response of VAMP4 (Fig. 6e-inset), although endocytic behavior of VAMP4 dominated on average (Fig. 6e). Strong endocytic behavior of VAMP4 was also consistent with its surface expression which equaled the size of the cytoplasmic VAMP4 pool (Supplementary Figure 7). The amounts of VAMP4 in all synaptic terminals were comparable, as judged by the fluorescence change in response to alkalinizing  $\text{NH}_4\text{Cl}$  treatment administered at the end of each experiment. This finding suggests that VAMP4 traffics independently without significant dynamic overlap with syb2 present in the same synaptic boutons. When taken together with robust rescue of evoked neurotransmission in syb2 deficient synapses (Fig. 2), these observations suggest that, in nerve terminals, VAMP4 simultaneously traffics to and from the plasma membrane in a activity-dependent manner (Fig. 6e), and that in a large number of synapses, the balance between VAMP4 exo- and endocytosis favors a net endocytic fluorescence change in pHluorin-based measurements. Interestingly, these experiments also indicate that vesicle populations that contain VAMP4 and syb2 show minimal overlap as the SNAREs manifest significantly distinct profiles of trafficking within individual presynaptic terminals.

## VAMP4 traffics independently of syb2

To assess the interaction between the pools of VAMP4 and syb2, we monitored VAMP4 trafficking in synapses lacking SNAREs required for exocytic fusion. In syb2-deficient synapses, VAMP4 fluorescence showed a net endocytic response akin to observations in wild type synapses (Fig. 7a, green and black traces). In the absence of syb2, VAMP4's endocytic response was more pronounced compared to VAMP4 retrieval observed in wild type neurons. This difference suggests that some fraction of VAMP4 exocytosis, hinted by the difference between the two endocytic responses, can be maintained by syb2.

Remarkably, however, the endocytic response of VAMP4 was significantly more accentuated in synapses lacking SNAP-25, the plasma membrane SNARE required for exocytosis of synaptic vesicles (Fig. 7a, grey trace). The net difference between VAMP4 endocytosis in syb2-deficient and SNAP-25 deficient synapses suggest the presence of a syb2-independent exocytic component of VAMP4 trafficking, which nevertheless requires SNAP-25, consistent with our earlier electrophysiological and biochemical results. To isolate this component of VAMP4 trafficking, we mutated a critical di-leucine motif present in the N-terminal region of VAMP4 (VAMP4 L25A) required for endocytosis and proper subcellular localization of VAMP4<sup>12</sup>. This mutation abolished evoked internalization of VAMP4 and uncovered a relatively modest but significant pool of VAMP4 that can traffic to the plasma membrane independent of syb2 (Fig. 7b). Interestingly, this mutated VAMP4 construct could still undergo endocytosis following exocytosis independent of the di-leucine motif, presumably via a mechanism that resembles syb2 endocytosis. This result agrees well with the selective rescue of asynchronous neurotransmission by wild type VAMP4 (Fig. 2) and suggests that exocytic trafficking is not a peculiarity of the VAMP4 L25A mutant, but shared with wild type VAMP4. Indeed, we could verify that similar to wild type VAMP4, the VAMP4 L25A mutant forms stable SNARE complexes with syntaxin1 and SNAP-25 (Supplementary Fig. 8) and maintains evoked neurotransmission when expressed on the background of syb2-deficient neurons (Supplementary Fig. 9).

To isolate the exocytic component of VAMP4 trafficking in wild type synapses, we used the membrane permeable high affinity vacuolar ATPase inhibitor folimycin, which blocks vesicle reacidification upon endocytosis and traps vesicles in an alkaline state, rendering pHluorin fluorescence insensitive to subsequent endocytosis<sup>23</sup>. Folimycin application uncovered a clear exocytic component within the pool of VAMP4-containing vesicles that predominantly show endocytosis (Fig. 7c). Moreover, dual color imaging experiments in the presence of folimycin confirmed that VAMP4 can support low levels of exocytosis in the same boutons that show robust syb2-mediated fusion (Fig. 7d). However, this analysis also revealed an apparent discrepancy between the amounts of VAMP4 exocytosis that can be detected using electrophysiological and optical measures. Nevertheless, it is plausible to expect that a very small amount of VAMP4 mobilization is sufficient to account for its direct role in exocytosis. This finding bolsters the notion that syb2 and VAMP4 both show exocytosis albeit with dramatically distinct kinetics and levels at individual boutons. Furthermore, these results suggest that, in nerve terminals, VAMP4 simultaneously traffics to and from the plasma membrane during activity thus maintaining vesicle fusion in addition to retrieval consistent with our electrophysiological observations (Fig. 2).

## VAMP4 dependent asynchronous release and VAMP4 endocytosis

How does the endocytic behavior of VAMP4 impact its function in execution of fusion? As indicated above, the VAMP4 L25A mutant forms stable SNARE complexes with syntaxin1 and SNAP-25 and maintains evoked neurotransmission. Therefore, the di-leucine-motif-dependent endocytosis of VAMP4 is not critical for maintenance of its exocytic function. Nevertheless, this rather unique property of VAMP4 may be required to create a supply of VAMP4 enriched vesicles following intense activity and subsequently accentuate asynchronous release. Next, we aimed to mimic this situation and test whether VAMP4 overexpression increases the propensity of asynchronous release following intense activity and whether di-leucine-motif-dependent VAMP4 recycling contributes to this process. When we challenged synapses expressing VAMP4 with 600 action potentials applied at 20 Hz and monitored recovery of synaptic responses during subsequent 1 Hz stimulation<sup>24</sup>, we detected a significant decrease in the rapid component of recovery typically observed within 1 sec (Fig. 8a). This inhibition of fast recovery required the di-leucine-motif of VAMP4 as expression of the VAMP4 L25A mutant supported rapid recovery. These results are consistent with the hypothesis that VAMP4 routes vesicles away from a rapid recycling pathway dominated by fast retrieval of syb2<sup>25</sup> thus inhibiting response recovery after intense stimulation. Moreover, VAMP4 overexpression significantly desynchronized the kinetics of the first evoked response after cessation of 20 Hz stimulation compared to controls (Fig. 8b–c). In contrast, VAMP4 L25A mutant expression blocked this gain-of-function effect and restored the synchronicity of synaptic responses after intense stimulation back to control levels. Taken together, these findings suggest a model where di-leucine-motif-dependent endocytosis VAMP4 leads to generation of VAMP4 enriched vesicles, which in turn mediate asynchronous release during intense activity (Supplementary Fig. 10).

## Discussion

The results we present in this study support a model where vesicle-associated SNARE VAMP4, functionally diverges from the key vesicular SNARE syb2 and predominantly maintains asynchronous release (Supplementary Fig. 10). This result is supported by a combination of approaches in electrophysiological experiments that document progressive desynchronization of release carried out by VAMP4 as well as optical recordings that show delayed exocytosis of VAMP4-tagged vesicles. This finding is in striking contrast to the complete functional interchangeability of syb2 with other vesicular SNAREs such as cellubrevin in the maintenance of synaptic neurotransmission<sup>18</sup>. The functional divergence of syb2 and VAMP4 appears to be encoded at the level of SNARE complexes formed by these two v-SNAREs. In comparison to the canonical SNARE complex formed by syb2, VAMP4-containing SNARE complexes do not readily interact with key constituents of fast synchronized release machinery, complexins and synaptotagmin 1, thus altering synchronicity and Ca<sup>2+</sup>-dependence of release. This difference in release properties can be driven by interactions with alternate Ca<sup>2+</sup> sensor(s) as it has recently been proposed for asynchronous release and spontaneous release<sup>26, 27</sup>. Our findings raise the possibility that molecular interaction partners of VAMP4-containing SNARE complexes may provide insight into novel mechanisms that regulate Ca<sup>2+</sup>-dependent release. A combination of electrophysiological gain-of-function and loss-of-function studies with optical imaging

experiments suggests that although some fraction of syb2 and VAMP4 are likely to be present on the same vesicle pool and traffic together to the surface membrane, a small but significant population of vesicles appears to be enriched in VAMP4, follows a distinct route of stimulation-dependent trafficking facilitated by VAMP4's N terminal di-leucine motif and selectively supports asynchronous release. It is surprising, however, that despite its robust ability to maintain evoked asynchronous release, VAMP4 expression in syb2-deficient synapses resulted only in a modest but significant increase in spontaneous release and VAMP4 knockdown only partially impaired the baseline levels of spontaneous transmission. These observations are consistent with the notion that asynchronous release and spontaneous release rely on partly independent mechanisms<sup>28, 29</sup>.

Previous studies had shown that repetitive activity at synapses can switch the mode of release from highly synchronous to asynchronous and that vesicles from the newly refilled readily releasable pool are more likely to fuse asynchronously<sup>30</sup>. These earlier results provide the basis for the notion that synchronous and asynchronous forms of release originate from the same pool of vesicles. Our findings do not exclude this possibility as the switch from synchronous to asynchronous release may occur due to formation of immature SNARE complexes during intense use<sup>31</sup> or via mobilization of vesicles that reside beyond the immediate vicinity of voltage-gated Ca<sup>2+</sup>-channels<sup>32</sup>. Both of these models do not require the distinct molecular and functional features of a non-canonical SNARE such as VAMP4. However, our findings point to an alternative pathway that involves activity-dependent generation of a synaptic vesicle population enriched in VAMP4. The VAMP4-dependent SNARE complex formed after recruitment of these vesicles can then provide a molecular substrate upon which an alternate Ca<sup>2+</sup> sensor acts to drive asynchronous release. In this way, sustained activity could shift the proportion of vesicles enriched in VAMP4 and desynchronize the kinetics of neurotransmitter release (see model in Supplementary Fig. 10). Although this molecular model suggests involvement of a distinct vesicle population, as generation of this vesicle pool requires activity, electrophysiological predictions of this model would still be compatible with earlier studies<sup>30</sup>. Therefore, it is important to note that the model we propose here is not mutually exclusive with the earlier models and may well represent one of several alternative means to initiate asynchronous release. Our proposal is also in line with the earlier finding that a mechanism intrinsic to the vesicle fusion machinery sets apart rapid and slow evoked neurotransmitter release<sup>33</sup>. Future studies investigating the properties of other vesicle-localized SNAREs<sup>9</sup> may test whether they also encode distinct forms of neurotransmission and form substrates for alternate regulatory pathways underlying release mode specific regulation of neurotransmission<sup>34</sup>. Indeed, recent work provided strong evidence that other synaptic vesicle associated SNAREs, VAMP7 and vti1a, preferentially support spontaneous release<sup>35, 36</sup>.

Accumulating evidence indicates that presynaptic nerve terminals harbor a molecularly heterogeneous population of vesicles that may drive distinct forms of neurotransmission with divergent kinetics and Ca<sup>2+</sup>-dependence<sup>23, 37, 38</sup>. In addition, there is also evidence that the route of synaptic vesicle recycling may differentially affect neurotransmission by generating vesicles with divergent propensities for fusion<sup>39-42</sup>. Furthermore, some nerve terminals, including those originating from CCK-containing inhibitory interneurons, have been shown to predominantly rely on asynchronous release mechanisms to regulate their

neurotransmitter output<sup>16, 43, 44</sup>. Our finding that VAMP4 selectively maintains asynchronous release and may be enriched in at least some terminals expressing CCK provides a potential molecular mechanism underlying these observations. Despite their immense analytical power, biochemical and proteomics studies provide information on the molecular composition of an “average” synaptic vesicle without significant insight into potential sources and mechanisms of structural and functional vesicle heterogeneity<sup>9, 45</sup>. Our results provide insight into how synapses may fine tune their neurotransmitter output by taking advantage of distinct vesicle-associated SNARE proteins with diverse functional properties.

## Methods

### Lentivirus construction

Lentiviral constructs expressing VAMP4 or syb2 were made in pFUGW transfer vector using standard molecular biology procedures and verified by sequencing.

### Production of recombinant lentiviruses

Lentiviruses were produced in HEK293T cell by cotransfection of pFUGW transfer vector and 3 packaging plasmids (pVsVg, pMdlg/pPRE and pRSV-Rev) using Fugene 6 reagent. One day after transfection, cells were exchanged into neuronal growth media and viruses were harvested after 48 hours of accumulation. Viral media was clarified by low speed centrifugation.

### Dissociated hippocampal cultures and lentiviral infection

Dissociated hippocampal cultures were prepared from syb2 or SNAP-25 knockout mice and their littermate controls or Sprague Dawley rats using previously published protocols<sup>5, 6</sup>. Neurons were infected at 4 days in vitro by adding 0.1 – 0.3 ml of viral media per coverslip in 24 well plates. All experiments were performed after 14 days in vitro to allow synapses to reach maturity<sup>46</sup>. All experiments were performed following protocols approved by the UT Southwestern Institutional Animal Care and Use Committee.

### RNAi knockdown

Oligonucleotides encoding rat VAMP4 shRNA sequences (TCGAGGATGATTTCAGATGAAGAAGTTC AAGAGACTTCTTCATCTGAATCATCTT A and CTAGTAAGATGATTTCAGATGAAGAAGTCTCTTGAACCTTCTTCATCTGAATCATCC for VAMP4 KD1; TCGAGGAGAATATTACCAAGGTAATTCAAGAGATTACCTTGGAATATTCTCTT A and CTAGTAAGAGAATATTACCAAGGTAATCTCTTGAATTACCTTGGAATATTCTC C for VAMP4 KD2) were inserted into the XhoI/XbaI cloning site downstream of the human H1 promoter in the L307 lentiviral transfer vector (gift of Dr. T. C. Südhof, Stanford). The efficiency of the knockdown was established by measuring the endogenous levels of VAMP4 mRNA in infected rat hippocampal neurons using quantitative real-time

PCR. VAMP4 knockdown in neuronal cultures was further verified by assaying endogenous VAMP4 using immunocytochemistry and Western blotting.

### Electrophysiology

Pyramidal neurons were voltage clamped to  $-70$  mV using an Axopatch 200B amplifier and Clampex 8.0 software (Molecular Devices), filtered at 2 kHz, and sampled at 5 kHz at room temperature ( $\sim 26^\circ\text{C}$ ). The pipette solution contained the following (in mM): 115 Cs-MeSO<sub>3</sub>, 10 CsCl, 5 NaCl, 10 HEPES, 0.6 EGTA, 20 tetraethylammonium chloride, 4 Mg-ATP, 0.3 Na<sub>2</sub>GTP, and 10 QX-314 (lidocaine N-ethyl bromide), pH 7.35 (300 mOsm). A modified Tyrode's solution used as the extracellular solution contained the following (in mM): 150 NaCl, 4 KCl, 2 MgCl<sub>2</sub>, 10 glucose, 10 HEPES, and 2 CaCl<sub>2</sub>, pH 7.4 (310 mOsm). The recordings were not corrected for the liquid junction potential ( $\sim 12$  mV). Under our recording conditions, we estimate the equilibrium potential for Cl<sup>-</sup> at  $-40$  mV; therefore, we could record inward inhibitory current without altering our standard pipette solution. To record and isolate IPSCs, the ionotropic glutamate receptor antagonist CNQX (10  $\mu\text{M}$ ; Sigma) and AP-5 (50  $\mu\text{M}$ ; Sigma) were added to the bath solution. To elicit evoked responses, electrical stimulation was delivered through parallel platinum electrodes in modified Tyrode's solution (duration, 1 ms; amplitude, 20 mA). The exchange between extracellular solutions was achieved by direct perfusion of solutions onto the field of interest by gravity. Spontaneous miniature IPSCs (mIPSCs) were recorded in the addition of 1  $\mu\text{M}$  tetrodotoxin (TTX). mIPSC events were identified with a 4 pA detection threshold and analyzed with Clampfit data analysis module (Molecular Devices).

### Fluorescence imaging

Hippocampal cultures were infected with lentivirus expressing the pHluorin or mOrange tagged constructs at 4 days in vitro and imaging experiments were performed after 14 days in vitro at room temperature ( $\sim 26^\circ\text{C}$ ). A modified Tyrode's solution containing 2 mM Ca<sup>2+</sup>, 10  $\mu\text{M}$  CNQX, and 50  $\mu\text{M}$  AP-5 was used in all experiments to block recurrent network activity. Baseline images were obtained every second for 30 s, and cultures were stimulated with field stimulation (duration, 1 ms; amplitude, 30 mA) as indicated above. For spectral imaging experiments shown in Figure 6 and Figure 7 images were obtained using a Carl Zeiss LSM 510 META laser-scanning microscope equipped with LSM 510 Laser module (Carl Zeiss). To optimize image acquisition settings, we obtained spectral signatures of pHluorin and mOrange probes when nerve terminals were either expressing each probe alone or both probes together. Analysis was performed at the level of individual synaptic puncta that were identified retrospectively after NH<sub>4</sub>Cl application to visualize the total pool of fluorescent proteins.

### Protein preparation and binding reactions

Plasmids encoding GST (glutathione S-transferase) fusion proteins with SNAP-25, syntaxin 1 (amino acids 1–261), syb2 (amino acids 2 – 94), and complexin 2 were described previously<sup>47, 48</sup>. Plasmids encoding GST fusion of VAMP-4 (amino acids 2 – 115) and its mutants were made using standard procedures and verified by sequencing. Mouse anti-synaptotagmin 1 (clone 41.1) and rabbit anti-complexin antibodies were from Synaptic Systems (Goettingen, Germany). Recombinant SNARE proteins were produced in BL21 E.

coli, and purified on glutathione–Sepharose beads (GE Healthcare). Beads were washed with buffer A (20 mM HEPES, 100 mM NaCl, 2 mM EDTA pH 7.3) and proteins were eluted either with 15 mM reduced glutathione (GSH) in buffer A or following thrombin cleavage<sup>48</sup>. Eluted proteins were purified further by size-exclusion chromatography on a Superdex 200 column (GE Healthcare) equilibrated in buffer A. The SNARE complexes were formed by mixing syntaxin-1, SNAP-25 and either Syb2 or VAMP4 for 30 min at 22°C in buffer A containing 0.8% octylglucoside. For pulldown reactions, 2 mcg of GST-tagged proteins were immobilized on glutathione-Sepharose beads for 1 hour at 4°C, and beads were incubated with proteins of interest for 30 min at 4 °C. Following a wash in buffer A containing 0.1% Triton X-100, bound material was analyzed by SDS-PAGE on 12% Ready gels (Bio-Rad). Brain extract was obtained as described<sup>48</sup>.

### Tissue preparation for immunohistochemistry

Mice were deeply anaesthetized (ketamine, 87 mg kg<sup>-1</sup>; xylazine, 15 mg kg<sup>-1</sup>) then transcardially perfused with ice-cold 100 ml 0.1 M phosphate-buffered saline (Sigma-Aldrich Canada). The perfusion was continued with 100 ml of phosphate-buffered saline with 4% paraformaldehyde (Sigma-Aldrich, Canada). The protocols were approved by the Animal Protection Committee of Université Laval. Brains were extracted and coronally sectioned at 50 µm (Vibratome, USA) and incubated for 24 h at 4°C with primary antibodies of interest. These included VAMP4 (from Synaptic Systems, Germany) and CCK (Santa Cruz Biotechnology, USA), primary antibodies were diluted, respectively, to 1: 100 and 1: 50, in 1% blocking solution. Tissue was rinsed and labelled with fluorescent secondary antibodies (Goat anti- rabbit Alexa Fluor 488, donkey anti-goat Alexa Fluor 546, (1:500) Invitrogen, Canada). Images were acquired with a FV1000 confocal microscope (Olympus).

### Electron microscopy

For electron microscopy VAMP4 was immunolabeled using Ultrasmall gold particles (F(ab')<sub>2</sub> Goat anti-rabbit UltraSmall Gold, 1:100; Electron Microscopy Science, Cat.# 25360), subsequently intensified with silver for better viewing (IntenSE M Silver Enhancement kit, Amersham, Cat# RPN 491). After osmification, samples were dehydrated by PLT (progressive-lowering of temperature) in a gradient of alcohol and embedded in Durcupan. Polymerisation of Durcupan was performed at 58° C. Samples were cut on a ultramicrotome UC7 (Leica Microsystems) at a thickness of 60 nm. Sections were retrieved on single slot copper grids coated with formvar. The sections were then contrasted with Reynold' s lead citrate stain. Observation were made on a Philips Tecnai 12 at an accelerating voltage of 100kV.

### Immunocytochemistry in neuronal cultures

2 – 3 week old high density hippocampal cultures were fixed in 4% paraformaldehyde for 15 minutes at room temperature and processed for immunocytochemistry essentially as described<sup>49</sup>. The following primary antibodies were used at 1:500 dilution: polyclonal anti-VAMP4 serum (Synaptic Systems), monoclonal anti-parvalbumin antibody (Millipore), monoclonal anti-synaptophysin I antibody (Synaptic Systems), polyclonal anti-synapsin antibody (gift of Dr T. Sudhof, Stanford). For detection we used Alexa-Fluor coupled secondary antibodies or in case of VAMP4 Alexa coupled tyramide amplification system

(Invitrogen). Stained coverslips were imaged on a Zeiss LSM510 confocal microscope using Zen 2009 software.

### Statistical analysis

Statistical significance between the experimental groups were assessed by one-way ANOVA-Fisher test at  $p < 0.05$ . For variance analysis, a Levene's test was used to determine the significant differences between the groups using a F value  $< 0.05$ .

### Supplementary Material

Refer to Web version on PubMed Central for supplementary material.

### Acknowledgements

We thank Mr. Jeremy Leitz for technical assistance as well as Drs. Helmut Kramer, Lisa Monteggia, Erika Nelson, and Elena Nosyreva for expert advice and discussions. We also thank Dr. Thomas C. Südhof for the gift of synaptobrevin2 knockout mice and Dr. Michael C. Wilson for the gift of SNAP-25 knockout mice. This work was supported by grants from the National Institute of Mental Health to E.T.K. E.T.K. is an Established Investigator of the American Heart Association.

### References

1. Sollner T, Bennett MK, Whiteheart SW, Scheller RH, Rothman JE. A protein assembly-disassembly pathway in vitro that may correspond to sequential steps of synaptic vesicle docking, activation, and fusion. *Cell*. 1993; 75:409–418. [PubMed: 8221884]
2. Jahn R, Lang T, Südhof TC. Membrane fusion. *Cell*. 2003; 112:519–533. [PubMed: 12600315]
3. Jahn R, Scheller RH. SNAREs--engines for membrane fusion. *Nat Rev Mol Cell Biol*. 2006; 7:631–643. [PubMed: 16912714]
4. Rizo J, Südhof TC. Snares and Munc18 in synaptic vesicle fusion. *Nat Rev Neurosci*. 2002; 3:641–653. [PubMed: 12154365]
5. Bronk P, et al. Differential effects of SNAP-25 deletion on Ca<sup>2+</sup>-dependent and Ca<sup>2+</sup>-independent neurotransmission. *J Neurophysiol*. 2007; 98:794–806. [PubMed: 17553942]
6. Schoch S, et al. SNARE function analyzed in synaptobrevin/VAMP knockout mice. *Science*. 2001; 294:1117–1122. [PubMed: 11691998]
7. Washbourne P, et al. Genetic ablation of the t-SNARE SNAP-25 distinguishes mechanisms of neuroexocytosis. *Nat Neurosci*. 2002; 5:19–26. [PubMed: 11753414]
8. Südhof TC, Rothman JE. Membrane fusion: grappling with SNARE and SM proteins. *Science*. 2009; 323:474–477. [PubMed: 19164740]
9. Takamori S, et al. Molecular anatomy of a trafficking organelle. *Cell*. 2006; 127:831–846. [PubMed: 17110340]
10. Bethani I, et al. Endosomal fusion upon SNARE knockdown is maintained by residual SNARE activity and enhanced docking. *Traffic*. 2009; 10:1543–1559. [PubMed: 19624487]
11. Steegmaier M, Klumperman J, Foletti DL, Yoo JS, Scheller RH. Vesicle-associated membrane protein 4 is implicated in trans-Golgi network vesicle trafficking. *Mol Biol Cell*. 1999; 10:1957–1972. [PubMed: 10359608]
12. Peden AA, Park GY, Scheller RH. The Di-leucine motif of vesicle-associated membrane protein 4 is required for its localization and AP-1 binding. *J Biol Chem*. 2001; 276:49183–49187. [PubMed: 11598115]
13. Geppert M, et al. Synaptotagmin I: a major Ca<sup>2+</sup> sensor for transmitter release at a central synapse. *Cell*. 1994; 79:717–727. [PubMed: 7954835]
14. Reim K, et al. Complexins regulate a late step in Ca<sup>2+</sup>-dependent neurotransmitter release. *Cell*. 2001; 104:71–81. [PubMed: 11163241]

15. Liu H, Dean C, Arthur CP, Dong M, Chapman ER. Autapses and networks of hippocampal neurons exhibit distinct synaptic transmission phenotypes in the absence of synaptotagmin I. *J Neurosci.* 2009; 29:7395–7403. [PubMed: 19515907]
16. Daw MI, Tricoire L, Erdelyi F, Szabo G, McBain CJ. Asynchronous transmitter release from cholecystokinin-containing inhibitory interneurons is widespread and target-cell independent. *J Neurosci.* 2009; 29:11112–11122. [PubMed: 19741117]
17. Chung C, Barylko B, Leitz J, Liu X, Kavalali ET. Acute dynamin inhibition dissects synaptic vesicle recycling pathways that drive spontaneous and evoked neurotransmission. *J Neurosci.* 2010; 30:1363–1376. [PubMed: 20107062]
18. Deak F, Shin O-H, Kavalali ET, Sudhof TC. Structural determinants of synaptobrevin 2 function in synaptic vesicle fusion. *The Journal of neuroscience : the official journal of the Society for Neuroscience.* 2006; 26:6668–6676. [PubMed: 16793874]
19. Maximov A, Sudhof TC. Autonomous function of synaptotagmin 1 in triggering synchronous release independent of asynchronous release. *Neuron.* 2005; 48:547–554. [PubMed: 16301172]
20. Chung C, Deak F, Kavalali ET. Molecular substrates mediating lanthanide-evoked neurotransmitter release in central synapses. *J Neurophysiol.* 2008; 100:2089–2100. [PubMed: 18715899]
21. Shaner NC, et al. Improved monomeric red, orange and yellow fluorescent proteins derived from *Discosoma* sp. red fluorescent protein. *Nat Biotechnol.* 2004; 22:1567–1572. [PubMed: 15558047]
22. Miesenbock G, De Angelis DA, Rothman JE. Visualizing secretion and synaptic transmission with pH-sensitive green fluorescent proteins. *Nature.* 1998; 394:192–195. [PubMed: 9671304]
23. Sara Y, Virmani T, Deak F, Liu X, Kavalali ET. An isolated pool of vesicles recycles at rest and drives spontaneous neurotransmission. *Neuron.* 2005; 45:563–573. [PubMed: 15721242]
24. Deak F, et al. Rabphilin regulates SNARE-dependent re-priming of synaptic vesicles for fusion. *Embo J.* 2006; 25:2856–2866. [PubMed: 16763567]
25. Deak F, Schoch S, Liu X, Sudhof TC, Kavalali ET. Synaptobrevin is essential for fast synaptic-vesicle endocytosis. *Nature cell biology.* 2004; 6:1102–1108. [PubMed: 15475946]
26. Groffen AJ, et al. Doc2b is a high-affinity Ca<sup>2+</sup> sensor for spontaneous neurotransmitter release. *Science.* 2010; 327:1614–1618. [PubMed: 20150444]
27. Sun J, et al. A dual-Ca<sup>2+</sup>-sensor model for neurotransmitter release in a central synapse. *Nature.* 2007; 450:676–682. [PubMed: 18046404]
28. Atasoy D, et al. Spontaneous and evoked glutamate release activates two populations of NMDA receptors with limited overlap. *J Neurosci.* 2008; 28:10151–10166. [PubMed: 18829973]
29. Xu J, Pang ZP, Shin OH, Sudhof TC. Synaptotagmin-1 functions as a Ca<sup>2+</sup> sensor for spontaneous release. *Nat Neurosci.* 2009; 12:759–766. [PubMed: 19412166]
30. Otsu Y, et al. Competition between phasic and asynchronous release for recovered synaptic vesicles at developing hippocampal autaptic synapses. *J Neurosci.* 2004; 24:420–433. [PubMed: 14724240]
31. Xu T, et al. Inhibition of SNARE complex assembly differentially affects kinetic components of exocytosis. *Cell.* 1999; 99:713–722. [PubMed: 10619425]
32. Sakaba T, Neher E. Quantitative relationship between transmitter release and calcium current at the calyx of held synapse. *J Neurosci.* 2001; 21:462–476. [PubMed: 11160426]
33. Wolfel M, Lou X, Schneggenburger R. A mechanism intrinsic to the vesicle fusion machinery determines fast and slow transmitter release at a large CNS synapse. *J Neurosci.* 2007; 27:3198–3210. [PubMed: 17376981]
34. Ramirez DM, Kavalali ET. Differential regulation of spontaneous and evoked neurotransmitter release at central synapses. *Curr Opin Neurobiol.* 2011; 21:275–282. [PubMed: 21334193]
35. Ramirez DM, Khvotchev M, Trauterman B, Kavalali ET. Vti1a identifies a vesicle pool that preferentially recycles at rest and maintains spontaneous neurotransmission. *Neuron.* 2012; 73:121–134. [PubMed: 22243751]
36. Hua Z, et al. v-SNARE Composition Distinguishes Synaptic Vesicle Pools. *Neuron.* 2011; 71:474–487. [PubMed: 21835344]

37. Fredj NB, Burrone J. A resting pool of vesicles is responsible for spontaneous vesicle fusion at the synapse. *Nat Neurosci.* 2009; 12:751–758. [PubMed: 19430474]
38. Rizzoli SO, Betz WJ. Synaptic vesicle pools. *Nat Rev Neurosci.* 2005; 6:57–69. [PubMed: 15611727]
39. Clayton EL, et al. Dynamin I phosphorylation by GSK3 controls activity-dependent bulk endocytosis of synaptic vesicles. *Nature neuroscience.* 2010; 13:845–851. [PubMed: 20526333]
40. Kavalali ET. Multiple vesicle recycling pathways in central synapses and their impact on neurotransmission. *The Journal of physiology.* 2007; 585:669–679. [PubMed: 17690145]
41. Virmani T, Han W, Liu X, Sudhof TC, Kavalali ET. Synaptotagmin 7 splice variants differentially regulate synaptic vesicle recycling. *The EMBO journal.* 2003; 22:5347–5357. [PubMed: 14532108]
42. Voglmaier SM, et al. Distinct endocytic pathways control the rate and extent of synaptic vesicle protein recycling. *Neuron.* 2006; 51:71–84. [PubMed: 16815333]
43. Hefft S, Jonas P. Asynchronous GABA release generates long-lasting inhibition at a hippocampal interneuron-principal neuron synapse. *Nat Neurosci.* 2005; 8:1319–1328. [PubMed: 16158066]
44. Iremonger KJ, Bains JS. Integration of asynchronously released quanta prolongs the postsynaptic spike window. *J Neurosci.* 2007; 27:6684–6691. [PubMed: 17581955]
45. Mutch SA, et al. Protein quantification at the single vesicle level reveals that a subset of synaptic vesicle proteins are trafficked with high precision. *J Neurosci.* 2011; 31:1461–1470. [PubMed: 21273430]
46. Mozhayeva MG, Sara Y, Liu X, Kavalali ET. Development of vesicle pools during maturation of hippocampal synapses. *J Neurosci.* 2002; 22:654–665. [PubMed: 11826095]
47. Bajohrs M, Rickman C, Binz T, Davletov B. A molecular basis underlying differences in the toxicity of botulinum serotypes A and E. *EMBO Rep.* 2004; 5:1090–1095. [PubMed: 15486565]
48. Hu K, Carroll J, Rickman C, Davletov B. Action of complexin on SNARE complex. *J Biol Chem.* 2002; 277:41652–41656. [PubMed: 12200427]
49. Ramirez DM, Andersson S, Russell DW. Neuronal expression and subcellular localization of cholesterol 24-hydroxylase in the mouse brain. *J Comp Neurol.* 2008; 507:1676–1693. [PubMed: 18241055]

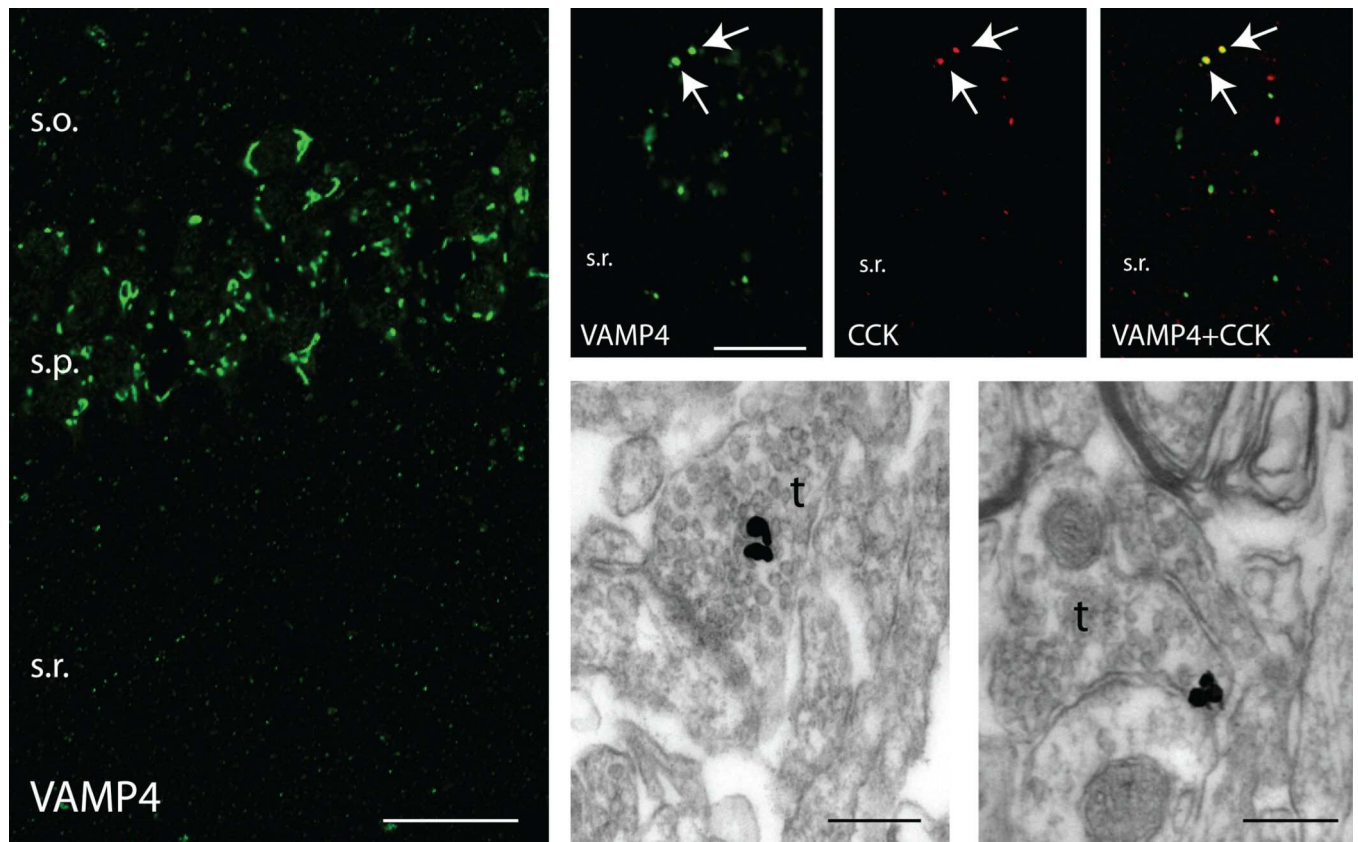


#### Figure 1. Synaptic localization of VAMP4

(a) Expression of VAMP4 in area CA1 of the hippocampus. Strong immunofluorescence is observed in the cell body layer (s.p. stratum pyramidale), consistent with VAMP4 localization in the Golgi apparatus. In addition, punctate staining is observed in every layer of the hippocampus including stratum radiatum (s.r.) and stratum oriens (s.o.). Calibration bar: 50  $\mu\text{m}$  (b–d) Double immunostaining with CCK demonstrates that VAMP4 is expressed in CCK-positive terminals in the str. radiatum (arrows). Calibration bar: 15  $\mu\text{m}$ . (e, f) Expression of VAMP4 in presynaptic terminals (t) is confirmed at the electron microscopic level using silver-enhanced immunogold particles. The absence of a clear postsynaptic density is consistent with this example being an inhibitory synapse Calibration bar: 200 nm.

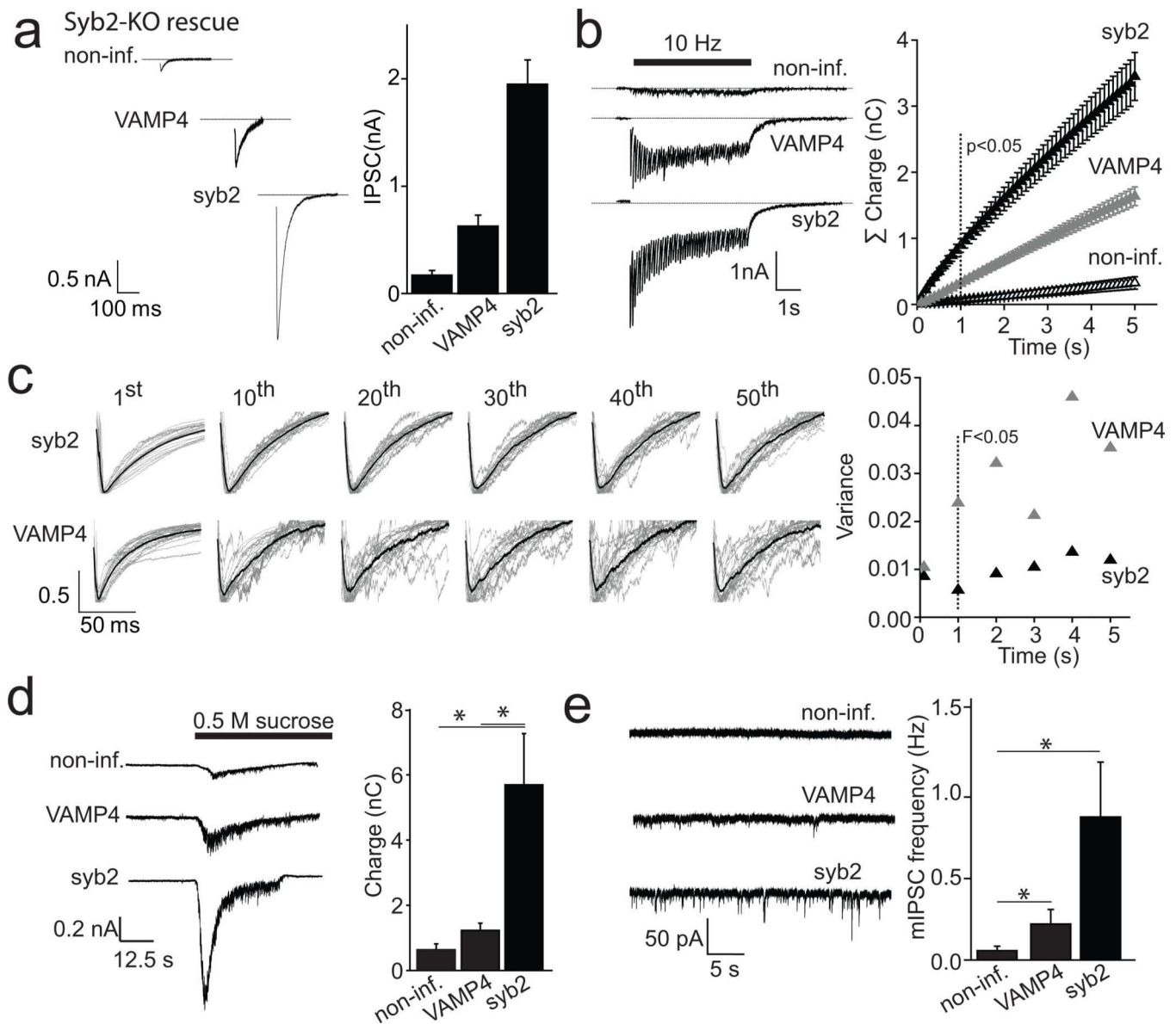


**Figure 2. VAMP4 mediates evoked asynchronous neurotransmitter release**

(a) Traces (left) and average peak values (right) of evoked IPSCs in uninfected syb2 deficient neurons ( $n=16$ ), or infected with VAMP4 ( $n=31$ ) or syb2 ( $n=35$ ). Here and in all subsequent figures bars represent mean  $\pm$  standard error of the mean (s.e.m.) and "\*" denotes statistical significance between the groups assessed by one-way ANOVA-Fisher test at  $p<0.05$ .

(b) (left) Response of the same cells shown in (a) to 50 action potentials (APs) triggered at 10 Hz. (Right) Average cumulative charge transfer of responses. Dotted line represents the time point at which the three groups begin to be statistically different.

(c) Normalized traces (gray) and average normalized traces (black) of the 1st, 10th, 20th, 30th 40th and 50th IPSC in a 10 Hz train of stimulation. The left graph displays the variance of the normalized current calculated for 0.5 ms, starting at 40 ms. Levene's test was used to determine the significant differences between the variances using a F value  $<0.05$  ( $n=24$ ).

The current values averaged between 40 and 40.5 ms are different only at the first IPSC, where the variance is not different.

(d) Representative traces (left) and mean charge transfer values integrated during the first 2 s of 30 s hypertonic stimulation (+0.5 M sucrose) (right) in non-infected syb2 deficient neurons (n=4 cells) or those infected with VAMP4 (n=6) and syb2 (n= 3).

(e) Representative traces (left) and average frequency (right) of mIPSCs in non-infected syb2 deficient neurons (n=5 cells) or those infected with VAMP4 (n=12) and syb2 (n=8).

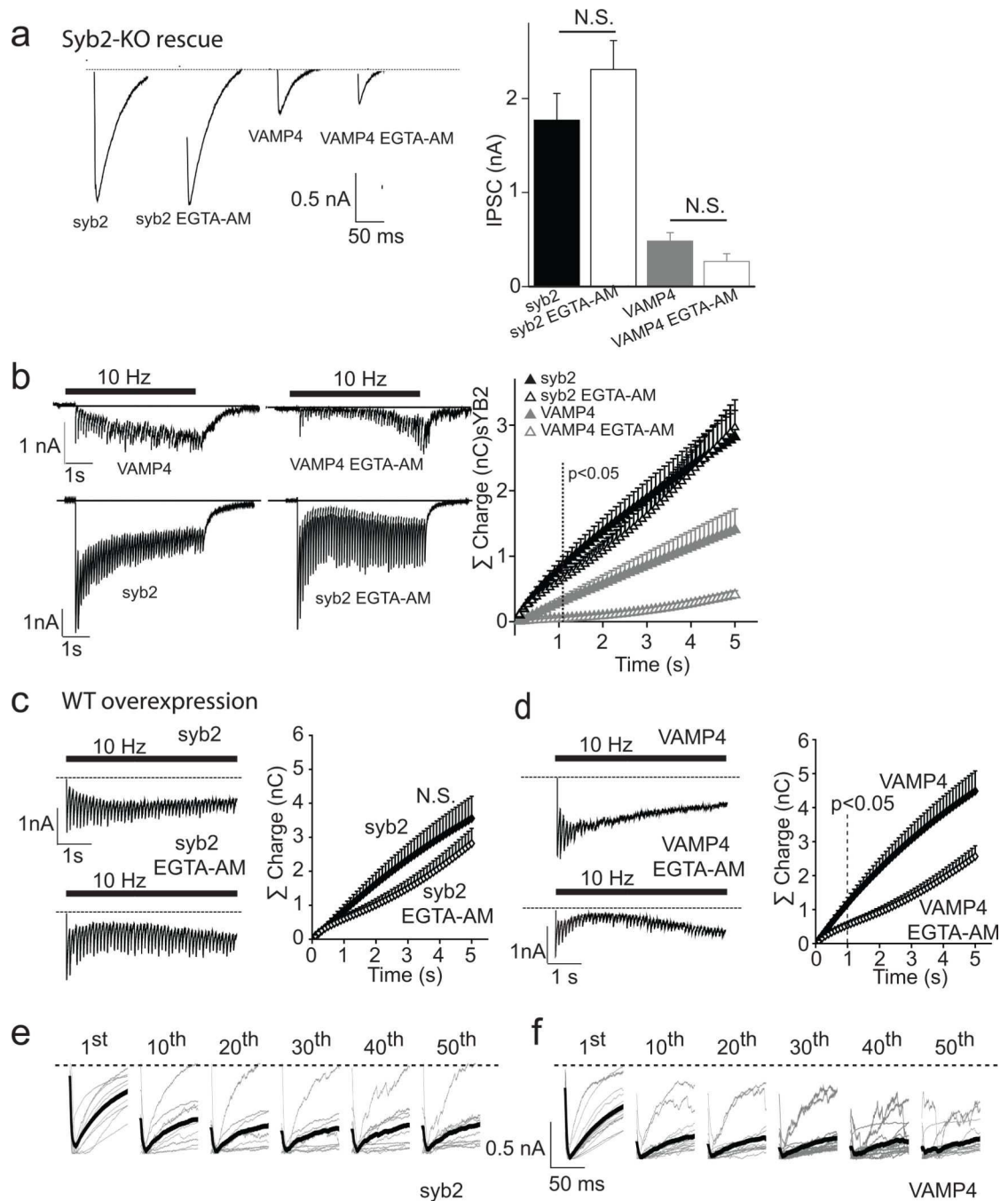


**Figure 3. VAMP4 mediated evoked neurotransmitter release is susceptible to slow  $\text{Ca}^{2+}$  buffering**

(a) Representative traces for IPSCs evoked by a single AP in syb2- or VAMP4-infected syb2 knockout neurons after pre-incubation in DMSO (vehicle) or EGTA-AM (10  $\mu$ M) ( $n=8$  for each group) for 10 minutes. N.S. denotes lack of significance.

(b) (Left) Representative traces for IPSCs evoked by 50 APs triggered at 10 Hz in syb2- or VAMP4-infected neurons after pre-incubation in DMSO (vehicle) or EGTA-AM ( $n=8$  for each group). (Right) Average cumulative charge transfer of responses. The gradual increase

is neurotransmission seen after EGTA-AM treatment is attributable to  $\text{Ca}^{2+}$  buffer saturation. Dotted line represents the time from which all groups are statistically different.

(c) (left) Representative traces of IPSCs evoked by 50 APs applied at 10 Hz in wild type hippocampal neurons overexpressing syb2 and pre-incubated with DMSO or EGTA-AM. (right) Average cumulative charge transfer values of IPSCs in neurons overexpressing syb2 and pre-incubated with DMSO or EGTA-AM (n=9 for each group). The difference between the two groups is not statistically significant at any time point.

(d) (left) IPSCs in neurons overexpressing VAMP4 under the same conditions as in c. (right) Average cumulative charge transfer values of IPSCs evoked by 50 APs at 10 Hz in neurons overexpressing VAMP4 and pre-incubated with DMSO (n=16) or EGTA-AM (n=14).

(e, f) Traces depict a progressive increase in asynchronicity of individual evoked IPSCs after VAMP4 overexpression compared to syb2 overexpression. Thick lines denote the mean of all traces depicted.

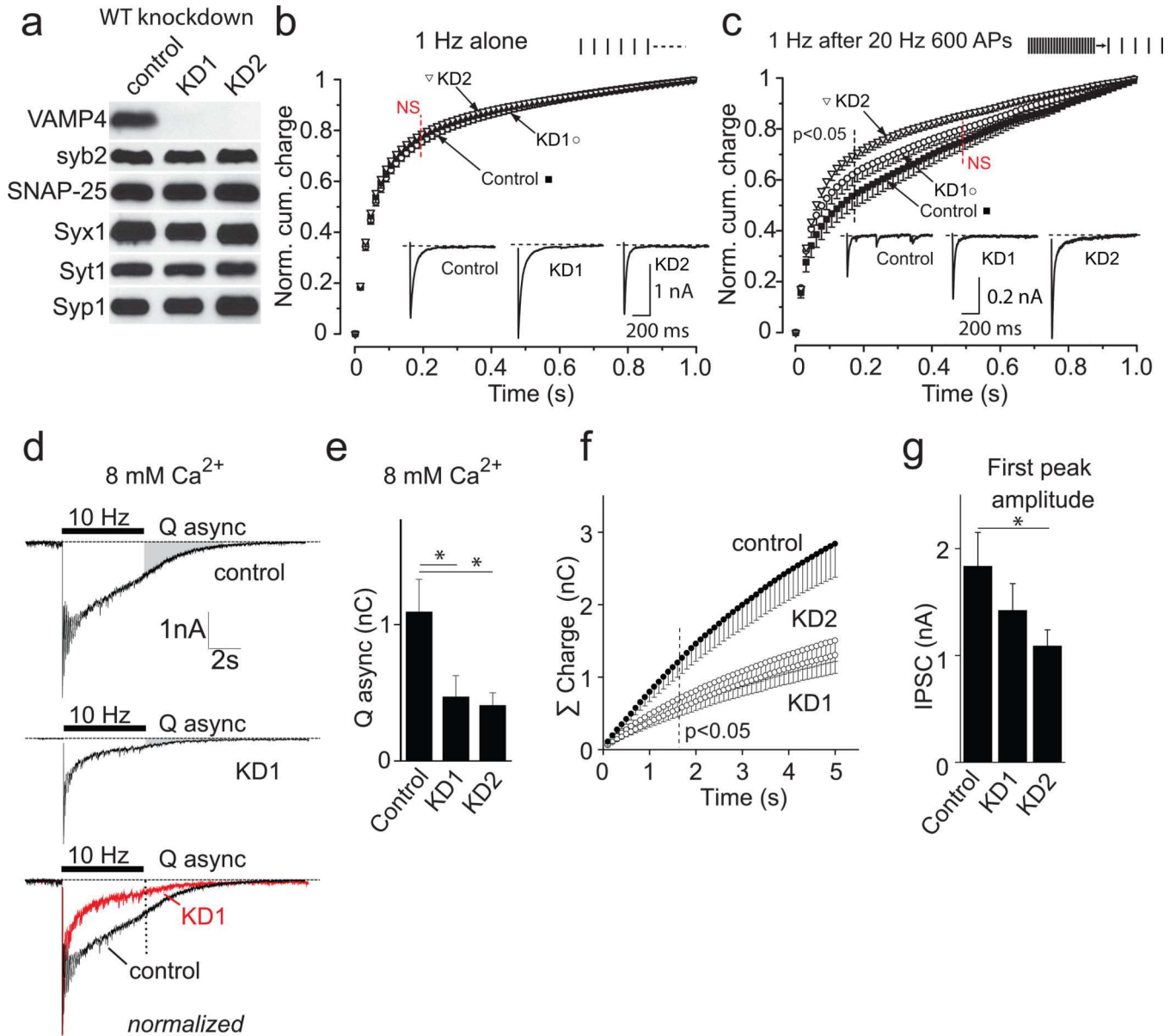


**Figure 4. VAMP4 loss-of-function attenuates the extent of asynchronous release**  
 (a) Immunoblot analysis of neurons pooled from 4 coverslips infected with L-307 virus (control) or VAMP4 knockdown viruses (KD1 and KD2). Syx1=Syntaxin 1; Syt1=Synaptotagmin 1; Syp1=Synaptophysin 1.  
 (b) Traces and average cumulative charge histograms (obtained from individual IPSC traces) depicting the synchronicity of synaptic responses during 1 Hz stimulation (in 2 mM Ca<sup>2+</sup>) after VAMP4 knockdown (control: n=11, KD1: n=15, KD2: n=12).  
 (c) The same analysis as in b performed on 1 Hz synaptic responses recorded after 600 APs at 20 Hz (control: n=15, KD1: n=11, KD2: n=12). Dashed line indicates statistical significance between VAMP4 knockdown (KD2) and control groups (p< 0.05). The difference between the KD1 group and controls was not significant (p=0.2).  
 (d) Normalized IPSC traces for 10 Hz stimulation in 8 mM Ca<sup>2+</sup> for Control, KD1, and KD2.  
 (e) Bar graph of Q async (nC) for Control, KD1, and KD2.  
 (f) Graph of cumulative charge (nC) over time (s) for Control, KD1, and KD2.  
 (g) Bar graph of IPSC first peak amplitude (nA) for Control, KD1, and KD2.

- (d) Late asynchronous release in the presence of 8 mM  $\text{Ca}^{2+}$  evoked by 50 APs applied at 10 Hz in rat hippocampal neurons infected with L-307 virus (control) or VAMP4 knockdown virus (KD1). Normalized traces depict the kinetic difference between the two groups.
- (e) Average charge transfer values of the late asynchronous release measured in 8 mM  $\text{Ca}^{2+}$  within 5 s after the cessation of 10 Hz stimulation in neurons infected with control (n=14), KD1 (n=12) or KD2 (n=11) viruses.
- (f) Average cumulative charge transfer for IPSCs in neurons infected with control (n=13), KD1 (n=11) or KD2 (n= 11) viruses. Dotted line represents the time point when the KD1 and KD2 groups are statistically different from control.
- (g) Average values of initial IPSC peaks measured in neurons infected with control (n=13), KD1 (n=11), KD2 (n= 11) constructs.

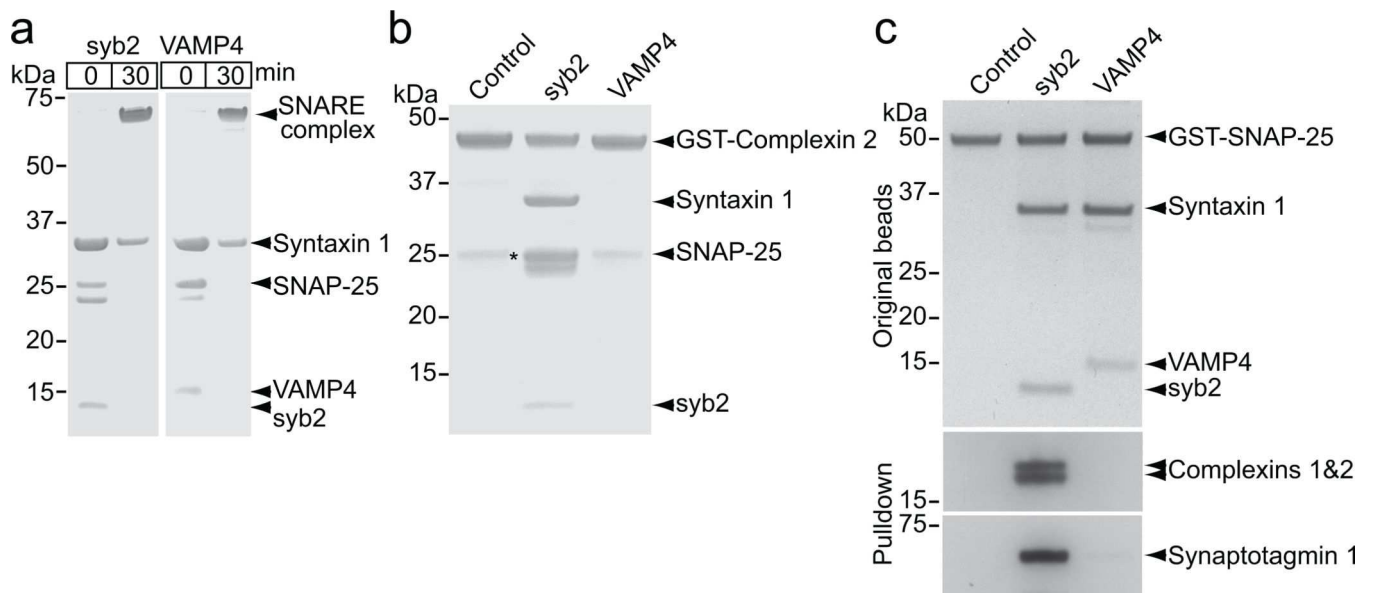


**Figure 5. The ternary complex of VAMP4 with syntaxin 1/SNAP-25 does not engage complexes or synaptotagmin 1**

(a) VAMP4 forms a stable SDS-resistant complex with Syntaxin 1 and SNAP-25 similar to syb2. Purified recombinant proteins (~5  $\mu$ M) were mixed and incubated for 30 min at 20°C and complex formation was visualized by PAGE and Coomassie staining.

(b) Complexin 2 binds syb2-, but not VAMP4-, containing ternary complex. GST-complexin 2 glutathione beads were incubated with the two preassembled ternary complexes and the bound material was visualized by PAGE and Coomassie staining. All samples were boiled prior to loading to disrupt the ternary complexes and reveal individual proteins. Asterisk indicates the GST tag alone present on the GST-complexin 2 beads. Note that recombinant SNAP-25 used in this study contained a minor proteolytic degradation product (second band slightly below 25 kDa).

(c) VAMP4 containing ternary complex does not bind endogenous complexes and synaptotagmin 1. GST-SNAP-25 (control) and VAMP4- or syb2-containing complexes were immobilized on glutathione beads via the GST-SNAP-25 protein (upper panel). Rat brain detergent extract was incubated with the beads for 1 hour at 4°C and, following washing, the bound material was visualized by immunoblotting (lower panel).

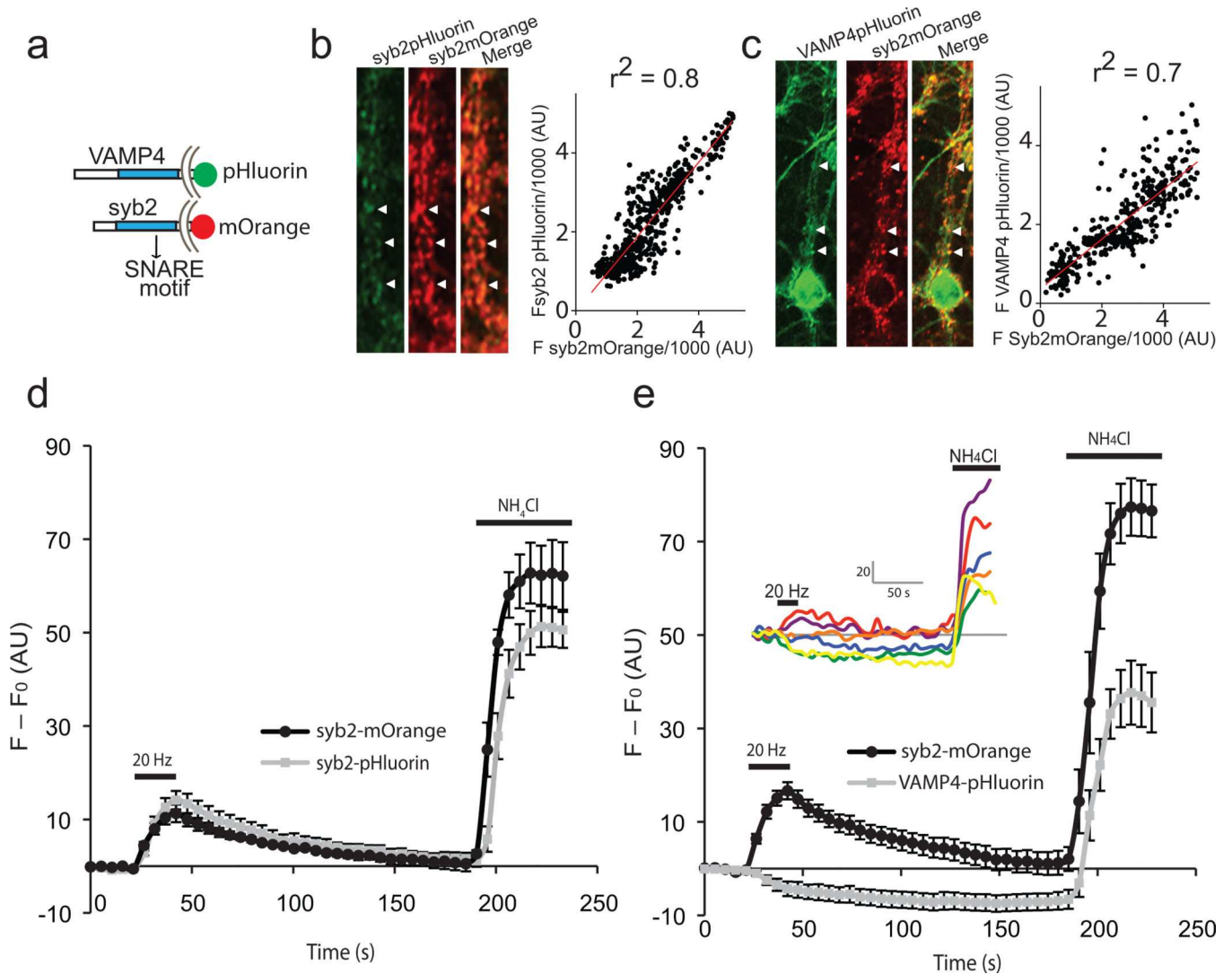


### Figure 6. Trafficking of VAMP4 at central synapses

(a) Schematic structures of VAMP4-pHluorin and syb2-mOrange constructs.

(b) (Left) Co-localization (arrows) of syb2-pHluorin and syb2-mOrange in hippocampal synapses after co-infection. (Right) The correlation between syb2-mOrange and syb2-pHluorin fluorescence in the presence of 50 mM  $NH_4Cl$  ( $n = 529$  synapses, 7 experiments).

(c) (Left) Co-localization of VAMP4-pHluorin and syb2-mOrange in hippocampal synapses after co-infection. (Right) The positive correlation between syb2-mOrange and VAMP4-pHluorin fluorescence in the presence of 50 mM  $NH_4Cl$  ( $n = 412$  synapses, 6 experiments).

(d) Average traces of syb2-mOrange and syb2-pHluorin fluorescence change at 282 individual boutons in response to 400 APs at 20 Hz followed by  $NH_4Cl$  treatment ( $n = 5$  experiments,  $p > 0.05$  difference between the groups is not significant).

(e) Average traces of syb2-mOrange and VAMP4-pHluorin fluorescence change at 798 individual boutons in response to 400 APs at 20 Hz followed by  $NH_4Cl$  treatment ( $n = 11$  experiments,  $p < 0.05$ ). Inset: VAMP4-pHluorin individual traces. VAMP4-pHluorin trafficking in response to 400 APs at 20 Hz at 5 different synapses. These traces demonstrate

the spectrum of stimulation-induced VAMP4-pHluorin trafficking from exo-endocytic or positive to endo-exocytic or negative.

Author Manuscript

Author Manuscript

Author Manuscript

Author Manuscript

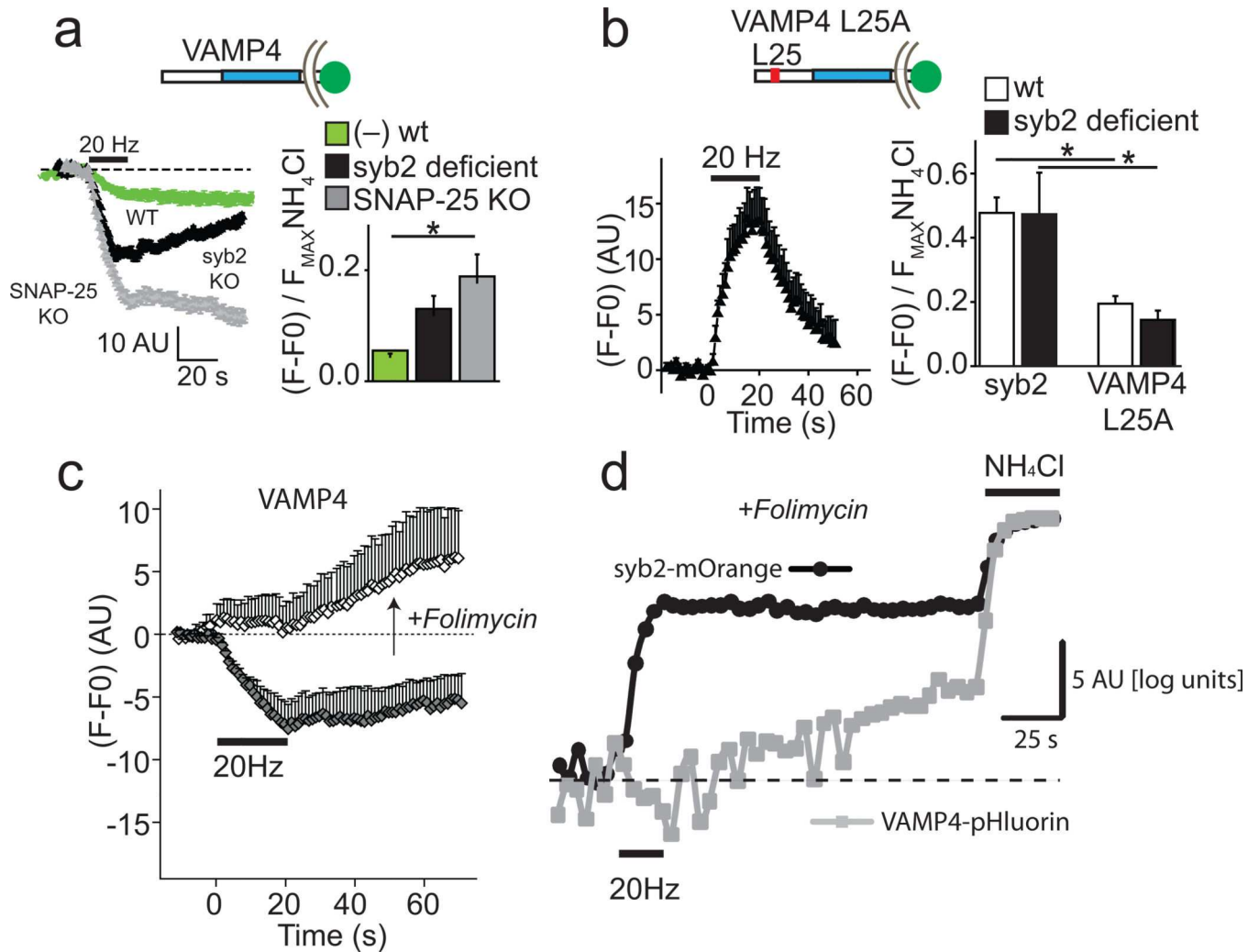


### Figure 7. VAMP4 traffics independently of syb2

- (a) VAMP4-pHluorin trafficking under stimulation (20 Hz for 20s) in wild type (green), syb2-deficient (black) and SNAP-25-deficient (gray) neurons. The bar graph shows the fraction of VAMP4 internalization in wild type (n=4), syb2-deficient (n= 6), and SNAP-25-deficient (n= 3) neurons. n denotes number of experiments.
- (b) VAMP4 L25A structure and its exo-endocytic trafficking under stimulation (20 s, 20 Hz) in syb2-deficient neurons. The bar graph shows the comparison of syb2-pHluorin and VAMP4 L25A-pHluorin exocytosis (as fluorescence increase) in wild type and syb2-deficient neurons (syb2: n= 12 wild type, n=7 syb2 deficient; VAMP4: n=3 wild type, n=7 for syb2 deficient). n denotes number of experiments.
- (c) Average traces of fluorescence change evoked by 400 APs applied at 20 Hz for boutons exhibiting VAMP4 trafficking before and after application of folimycin (n=4 experiments).
- (d) Dual color imaging experiments in folimycin indicate that VAMP4 can support low levels of exocytosis in the same boutons that show robust syb2-mediated fusion (n=40 boutons).

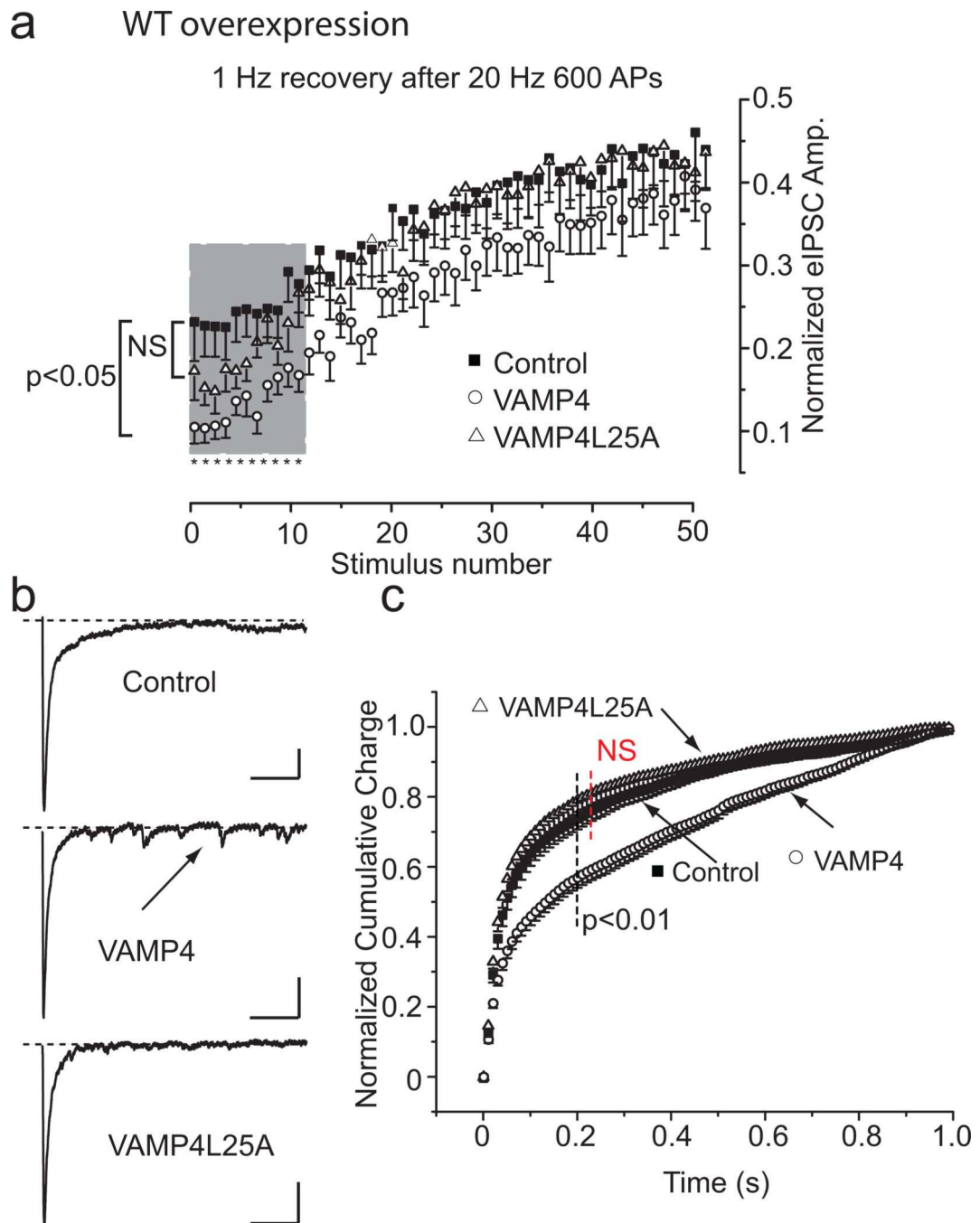


**Figure 8. VAMP4 trafficking enables asynchronous release during intense activity**

(a) Recovery of synaptic responses during 1 Hz stimulation after 600 action potentials applied at 20 Hz in control ( $n=15$ ), VAMP4 overexpressing ( $n=12$ ) and VAMP4 L25A ( $n=10$ ) expressing neurons. These experiments followed the same setting as in Fig. 3. Shaded area denotes the region where synaptic responses between control and VAMP4 overexpressing neurons are significantly different ( $p < 0.05$ ). In contrast, the same comparison between control and VAMP4 L25A expressing neurons did not reveal statistical significance ( $p > 0.05$ ).

(b) Representative traces depicting desynchronized synaptic responses triggered after intense stimulation in synapses overexpressing VAMP4. This desynchronization of release was attenuated after expression of VAMP4 L25A mutant. Bar graphs 200 ms vs. 50 pA.

(c) Cumulative charge averaged from multiple experiments depicting the desynchronization of synaptic responses after intense activity in synapses expressing VAMP4. Dashed line indicates statistical significance between VAMP4 and control groups. In contrast, VAMP4 L25A expressing synapses did not show statistical difference with respect to controls.